

# STUDY ON THE SETTLEMENT LAW OF TUNNEL IN DIATOMITE STRATUM BASED ON STRAIN SOFTENING MODEL

*Yan Li<sup>1</sup>, Huijian Zhang<sup>2</sup>, Gongning Liu<sup>2,\*</sup>, Yuchao Zheng<sup>2</sup>, Wei Fang<sup>1</sup>, Lichuan Wang<sup>3</sup>*

1. China Railway Design Corporation, Tianjin, Hebei District, 300000, China; liyan@crdc.com; 2876568700@qq.com
2. Southwest Jiaotong University, Key Laboratory of Transportation Tunnel Engineering, Ministry of Education, Chengdu, No. 111, North Section, Second Ring Road, Jinniu District, 610031, China; huijianz@163.com; yczh@home.swjtu.edu.cn; 2995484603@qq.com
4. China Railway 18th Bureau Group Co., Ltd., Tianjin, 300222, China; wlc773747@126.com

## ABSTRACT

Nowadays, there is no precedent for building a high-speed railway in diatomite area. Due to the complex structure and poor mechanical properties of diatomite as well as the lack of relevant engineering experience, more attention has been paid to the proper constitutive model of the tunnel in diatomite layer using the numerical calculation method, while the traditional Elastoplastic calculation model is the most used yet. Therefore, relying on the Feifengshan tunnel, through FLAC<sup>3D</sup> software as well as the on-site monitoring, the analysis of the settlement law about tunnelling in diatomite stratum is carried out based on different constitutive models. The research results show that diatomite has obvious strain-softening characteristics. The calculated surface settlement and vault settlement based on the Strain Softening model is greater than that based on the Mohr Coulomb model. When compared with the on-site monitoring data, it is found that the Strain Softening model would more accurately show the settlement law of the tunnel in diatomite and has better applicability in the diatomite area. The above-mentioned research results may provide some references for the construction and design of tunnels in similar strata in the future.

## Keywords

Diatomite, Strain-softening model, Tunnelling, Settlement, On-site monitoring

## INTRODUCTION

Diatomite is a kind of sedimentary rock formed by the remains of single-celled algae after many years of deposition. It has the characteristic of large pores, low density, loose structure, well-developed joint, and large compressibility, it softens easily when in contact with water and the mechanical abilities will decrease sharply [1, 2]. Han [3] analyzed the engineering characteristics of diatomite based on field experiments, and compared the reinforcement effects of different pile types in diatomite area. Existing studies mainly focused on the selection of subgrade reinforcement in diatomite area, and evaluated the applicability of reinforcement scheme to diatomite geology from the perspective of pile forming effect, bearing capacity and construction, and selected the optimal reinforcement measures according to the comparison of test results [4-6]. Based on the calculation model and triaxial test of diatomite, the test results were compared with numerical simulation calculation, and it showed that the diatomite had obvious strain-softening characteristics [7-9]. In the research of tunnels in soft rock, the traditional Mohr-Coulomb model was often selected as the constitutive model when the numerical simulation method was used [10-15]. Nam and Bobet [16]

studied the variation law of the deformation amplitude of a circular tunnel using an elastic model and proposed corresponding analytical solutions. Wang and He [17] revealed the influence of the lining type and the stress release rate before the preliminary lining on the stability about tunnel, and proposed the related measures, such as systematic bolt or shotcrete lining, grouting after installation of preliminary lining, and 20% of stress release rate before the installation of preliminary lining.

It was found that many geotechnical materials had strain-softening characteristics, and the impact about the strain-softening characteristics on stability about tunnel should be considered [18]. Gao et al. [19] studied the difference in the contribution rate of advance reinforcement and preliminary lining on the control effect of the surface settlement of shallow-buried tunnels in diatomite. Zhao et al. [20] focused on the impact about parameter of strain-softening model on deformation of tunnel, and found the Elastic Modulus, Poisson's ratio as well as softening modulus had great influence on the tunnel deformation. The application of the strain-softening model in tunnel engineering was analysed adopting Hoek-Brown strength criterion, and some references for the optimization as well as stability analysis of the tunnel engineering were also provided [21-24]. The mechanical parameter about Mohr-Coulomb model used in the FLAC3D software is pre-set as constants, which not perfectly show the softening effect about surrounding rock led by the decrease in the strength parameter about surrounding rock in nonlinear phase [25]. With the rapid development of computing software, the strain softening phenomenon of rock mass can be well simulated, and the proposed strain softening constitutive model also provides an important reference for solving engineering problems [26, 27]. However, due to the differences in engineering properties of different soil qualities, the existing research results cannot be simply applied to guide engineering practice in diatomite. Also, there is no precedent for the construction about high-speed tunnel in diatomite before this project. For the numerical calculation of tunnel in diatomite, it is necessary to study the applicability of suitable constitutive models to the construction mechanics of tunnel in diatomite, which plays a vital role in guiding engineering practice.

Therefore, relying on the Feifengshan tunnel of the Hangzhou-Shaoxing-Taizhou Railway, on-site test about diatomite is carried out, and numerical calculation is also taken on for the tunnel in diatomite adopting different constitutive models. Then the calculation results difference is compared and analysed, and a proper constitutive model with better applicability is obtained through the comparison of on-site monitoring. The findings may be good references for the designing as well as construction about tunnels in similar strata in the future.

## **MECHANICAL CHARACTERISTICS OF DIATOMITE BASED ON THE ON-SITE DIRECT SHEAR TEST**

### **Engineering background**

In this paper, the Feifengshan tunnel of the Hangzhou-Shaoxing-Taizhou Railway is taken as the supporting project, and the tunnel is mainly in diatomite stratum. The tunnel width is about 9.0m, the clearance height is about 6.2m and the clearance area is 43.2m<sup>2</sup>. The preliminary linings are made of C25 concrete and steel arch lining with a thickness of 23cm; secondary linings are made of C30 reinforced concrete with a thickness of 40cm, the detail is shown in Fig. 1. To further study the mechanics about diatomite, the on-site direct shear test about diatomite is further carried out on site.

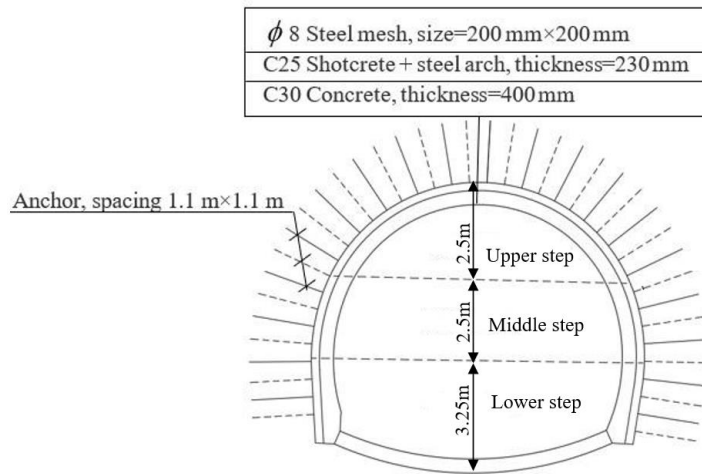
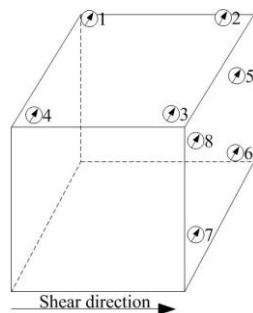


Fig. 1 - Design section about tunnel

### On-site direct shear test of diatomite

The on-site shear test is conducted on a section of Feifengshan Tunnel, and a total of six specimens are tested. The size of each specimen is 50cm×50cm×50cm (the shearing area is 0.25m<sup>2</sup>). During the test, a steel shear box with the same size as the specimen is used to fix the specimen. The normal force and shear force are applied by hydraulic jacks that are independent of each other, and the external reaction force device is loaded with sandbags. The measuring equipment for shear displacement and normal displacement is dial indicators, and the layout is presented in Figure 2. The normal displacement about specimen is the average value of indicators 1~4 and the shear displacement of the specimen is the average value of indicators 5~8. The purpose of this test is to obtain the on-site shear strengths of diatomite as a function of the normal stress on the shear face. The specimens are applied respectively with normal loads of 200kPa, 320kPa, 480kPa, and 680kPa.



(a) Position of the dial indicator



(b) On-site dial indicator installation

Fig. 2 - Schematic diagram layout of the dial indicators

When the quick shear method is adopted in the test, the vertical loads are applied once, and the shear load is applied immediately. When the quick consolidation shear method is used for the test, the normal load is usually added to the predetermined load evenly in 4 to 5 grades, and then the normal stress remains unchanged. After each grade of the load is applied, the vertical deformation value should be measured immediately, then measured and recorded once for every 5 minutes. When the vertical deformation value does not exceed 0.05mm within 5 minutes, the next level of load is applied. After the last level of load is applied, the vertical deformation value is measured at the intervals of 5min, 10min, 15min, and 15min. When the cumulative value of vertical deformation for two sets of 15mins does not exceed 0.05mm, the vertical deformation value is

considered to stable and the shear load can be applied. The shear force is applied using the incremental loading method after the normal load is kept constant. It is usually applied gradually (at least in 10 steps) uniformly according to the estimated shear strength grades to control the shear displacement rate. At least 10 sets of readings are usually taken before the specimen reaches actual shear strength. When the peak value of shear stress is reached or the shear deformation increases sharply or the shear deformation is greater than 1/10 of the diameter (or side length) of the specimen, it is considered that the shear failure has occurred and the test can be stopped. The on-site direct shear test process and shear face are shown in Figure 3, and the corresponding shear force-shear displacement curve of the diatomite is presented in Figure 4.

As shown in Figure 4 that when the confining pressure is 200 kPa~680kPa, the diatomite all exhibits obvious “strain-softening” characteristics. During the elastic stage, shear force-shear displacements under different confining pressures all show a linear relationship, that is, the shear displacement increases with the shear force, and the difference between the slopes of different confining pressures is small. In the softening stage, the specimen fails when the shear displacement peak appears, the shear force gradually decreases, while the shear displacement continues to increase. In the residual stage, the shear force gradually decays and reaches a stable value, and the value fluctuation is small, but the shear displacement continues to accumulate.



(a) Test specimen



(b) Test loading



(c) Shear face

*Fig. 3 - Test process of the diatomite*

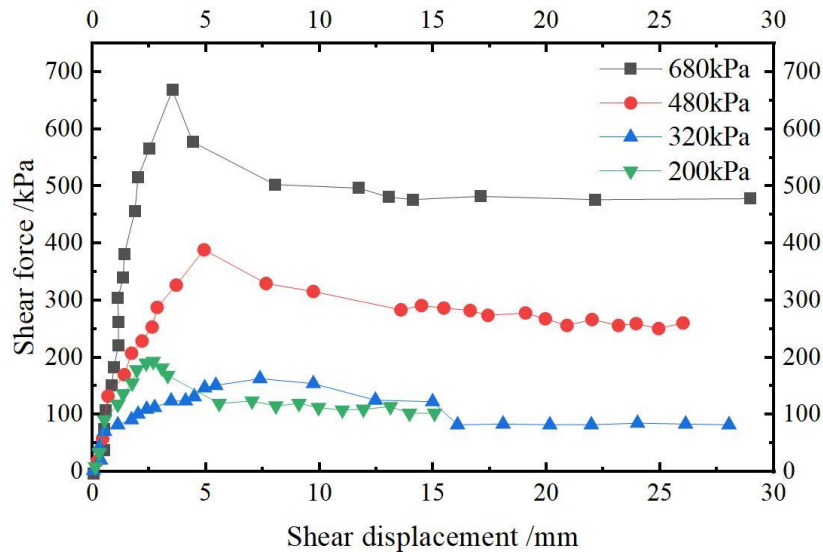


Fig. 4 - Shear force-shear displacement curve of the diatomite under different confining pressures

## NUMERICAL SIMULATION ANALYSIS OF TUNNEL IN DIATOMITE BASED ON DIFFERENT CONSTITUTIVE MODELS

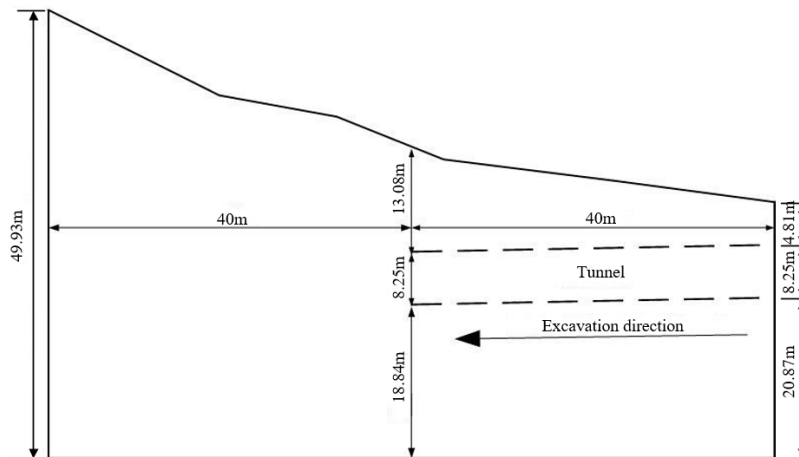
From the findings about on-site direct shear test of diatomite in the previous section, it can be found that the diatomite has obvious strain-softening characteristics. In practice, due to the limitation of test conditions, numerical simulation has gradually become an important means of the research. In this section, the numerical calculation method is used to further analyze the suitable constitutive model for diatomite, aiming to supply some reference for the tunnel with similar strata in the future.

### Numerical calculation model

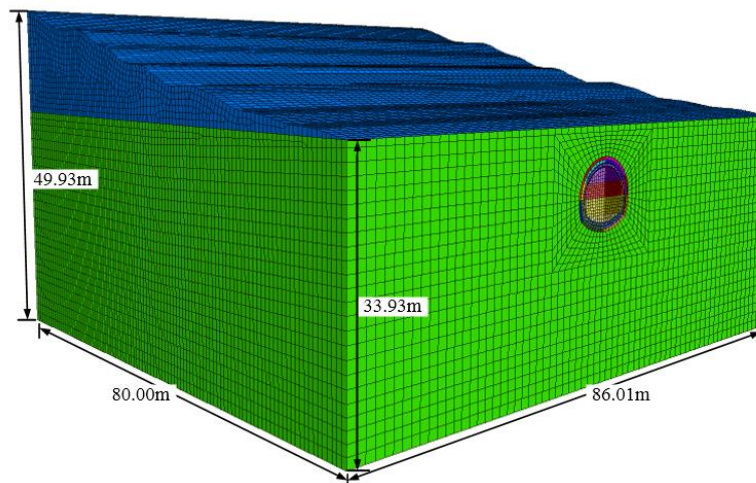
#### Calculation instruction

FLAC3D is adopted for the research. According to the theory about tunnel mechanics, the impacting ranges of tunnel's construction on surrounding rock are limited. When the distance is five times the tunnel diameter, then the calculation result error is less than 1%, and when the distance is three times the tunnel diameter, the calculation result error is less than 5%. Therefore, the boundary on the left-right sides about model is taken as 4 times the tunnel diameter. The dimension is presented in Figure 5(a) and the longitudinal excavation length is 40m.

To better simulate the calculation effect and reduce the boundary effect of the rear section [28, 29], the tunnel model extends 40m outward at the exit section (namely the longitudinal length is 80m). The model has a total of 308070 nodes and 296362 elements. The meshing diagram is shown in Fig. 5(b). Normal constraint is added to the front, rear, left, as well as right boundaries about model, and the bottom boundary is fixed [30]. The self-weight load is considered and the acceleration of gravity is taken as  $10\text{m/s}^2$ . Three-bench excavation method is adopted to simulate excavation process as the real project.



(a) Model size



(b) Mesh division

Fig. 5 - Numerical model

### Calculation parameter

Both the preliminary lining and secondary lining adopt solid element and follow the linear elastic criterion. The surrounding rock is diatomite, and its calculation parameter is selected based on geological survey data, as presented in Table 1. To improve the calculation efficiency, the lining effect about steel arch will be simulated by the equivalent method, namely, the elastic modulus about steel arch as well as steel mesh is converted into concrete.

Tab. 1 - Calculation parameters about surrounding rock and lining structures

Material type	Elastic Modulus $E$ /MPa	Poisson's ratio $\mu$	Density $\gamma$ /( $\text{kN/m}^3$ )	Cohesion $c$ /kPa	Internal friction angle $\varphi$ / $^\circ$
Surrounding rock	37.7	0.35	16.2	60.4	25.8
Anchor	200000	0.30	78.5	-	-
Preliminary lining	25500	0.30	25.0	-	-
Secondary lining	32000	0.30	25.0	-	-

### Analysis of the constitutive model

It is assumed that the constitutive model about diatomite layer is the Mohr Coulomb (MC) model or Strain Softening (SS) model, and the analysis of numerical calculation about tunnel in diatomite is conducted.

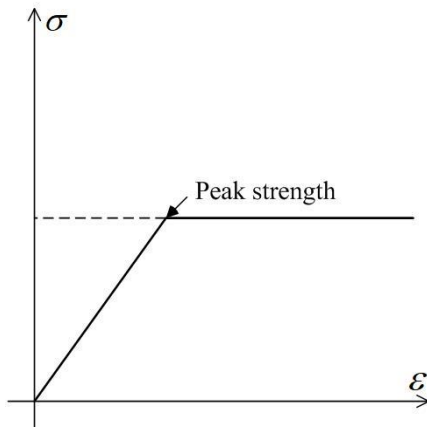


Fig. 6 - MC model

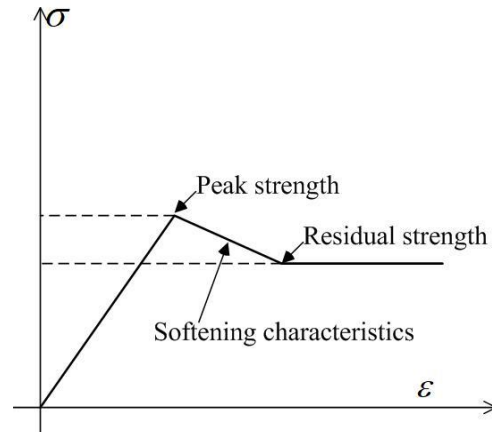


Fig. 7 - SS model

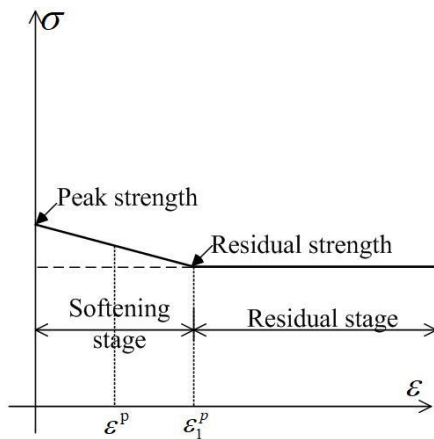


Fig. 8 - Reduction curve of the strength parameter

The curve of the MC model is presented in Figure 6, the curve of the SS model is presented in Figure 7, and the reduction curve about strength parameter is presented in Figure 8 (i.e., the detail of the curve after the peak strength in Figure 7). Obviously, the SS model is the special form about MC model. The difference is that the strength of the SS model will weaken after the plastic change begins. In FLAC3D software, the piecewise function of different strength parameters can be pre-set to represent the strain-softening phenomenon about material strength after the SS model enters the plastic stage, while the Mohr Coulomb model does not consider this weakening process. In FLAC 3D, the corresponding cohesion  $c$  and internal friction angles of different plastic shear strains can be preset in the table, so as to show the strain softening phenomenon of materials after plastic deformation. Therefore, the SS model is used as the calculation method (as shown in Figure 8) to express the softening phenomenon of material strength.

Taking cohesion as an example, its calculation equation is as followings after entering the strain-softening stage:

$$c = \begin{cases} c_0 \left[ 1 - \frac{(1 - \eta_c) \varepsilon^p}{\varepsilon_1^p} \right], & (0 \leq \varepsilon^p \leq \varepsilon_1^p) \\ c_0 \eta_c, & (\varepsilon^p \geq \varepsilon_1^p) \end{cases} \quad (1)$$

Where:  $\varepsilon^p$  is the plastic shear strain;  $\eta_c = c_{cr} / c_0$  is the cohesion reduction rate, which reflects the degree of strength reduction after the peak;  $\varepsilon_1^p$  is the critical plastic softening coefficient, i.e., the plastic shear strain at the junction of the softening stage and the residual stage [25].

### Calculation of strain-softening parameter

The key of strain softening model is to determine the law of strength parameter changing with the development of cumulative plastic shear strain [31]. The relationship between residual strength and peak strength and cumulative plastic shear strain can be determined by the direct shear test. Based on the direct shear test result of the third institution in the relying engineering project of this paper [32], using the least square method to fit the load and shear stress, the shear strength indexes of the tunnel in diatomite are obtained, as shown in Table 2. The cohesion reduction rate is  $\eta_c = 48/105 = 0.457$ , and the reduction rate of internal friction angle is  $\eta_\phi = 35/41 = 0.854$ . The test also shows that the specimen typically undergoes three stages during the shearing process, and the typical shear force-shear displacement curve obtained from the on-site direct shear test is presented in Fig. 9. In Fig. 9, the plastic shear strain generated in the softening stage is  $\gamma^p = L_{AB} / R = 8.63/500 = 0.01726$ ,  $R$  is the specimen diameter, taken as the field specimen size (namely, 500mm).

Tab. 2 - In situ direct shear test results of diatomite

Name	c/kPa	$\phi/^\circ$
Peak strength	105	41
Residual strength	48	35

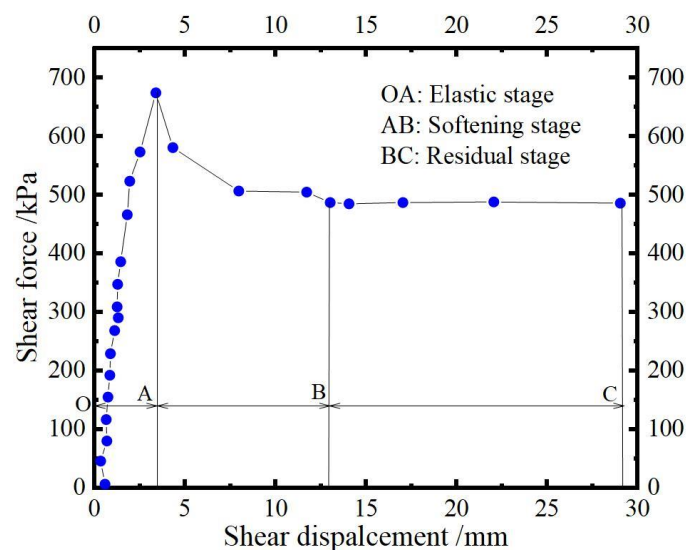


Fig. 9 - The relationship between the shear force and the shear displacement about diatomite



According to the literature [33], the relationship between the critical plastic softening coefficient  $\varepsilon_1^p$  and  $\gamma^p$  in FLAC<sup>3D</sup> is:

$$\varepsilon_1^p = \frac{\sqrt{3}}{3} \cdot \frac{\sqrt{1+K_\psi + K_\psi^2}}{1+K_\psi} \cdot \gamma^p \quad (2)$$

Where  $K_\psi = \frac{1+\sin\psi}{1-\sin\psi}$ ,  $\psi$  is the dilatancy angle of the soil. According to Eq. (2), when  $\psi = 0$ ,  $\varepsilon_1^p = \frac{\gamma^p}{2}$ ; even when  $\psi$  is very large, the relationship between  $\varepsilon_1^p$  and  $\gamma^p$  is close to the case of  $\psi = 0$ . Therefore,  $\varepsilon_1^p = \frac{\gamma^p}{2} = 0.01726/2=0.00863$  is taken in this paper.

## Settlement law about tunnel in diatomite under different constitutive models

### Surface settlement

The variation of surface settlement (10m, 20m, and 30m section away from the entrance of the tunnel) with excavation steps is shown in Figure 10.

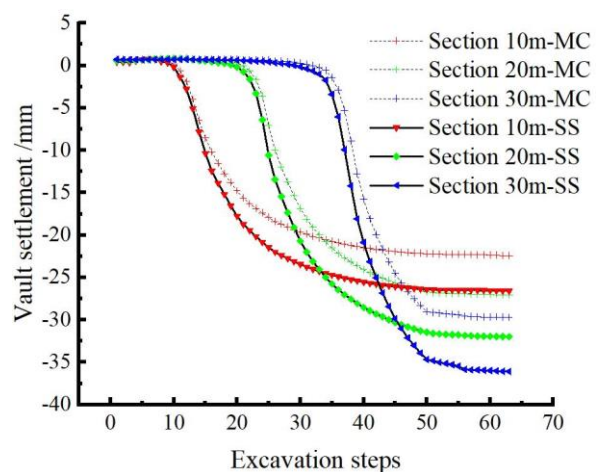
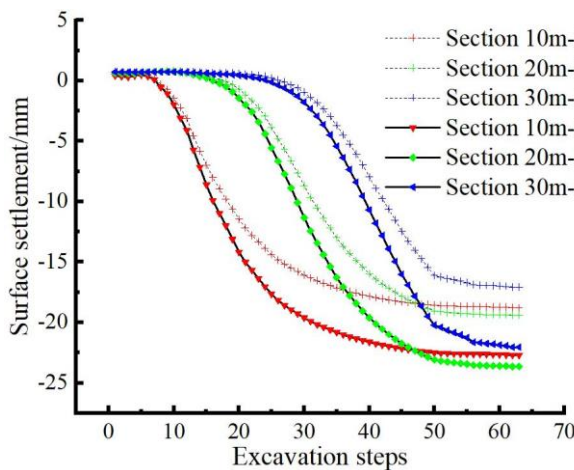


Fig. 10 - Variation curve about surface settlement with excavation step Fig. 11 - Variation curve about vault settlement with excavation steps for each section

In Figure 10, the surface settlement trends under the two constitutive models are basically the same in a whole. When the tunnel excavation face has not been excavated to the vicinity of the target section, the surface settlement of the target section has not changed significantly. When the tunnel excavation face excavates to the vicinity of the target section, a large settlement occurs on the surface and it develops rapidly. With the increasing distance of the excavation face, the disturbance to the surface of the target section by the excavation face gradually decreases, and the surface settlement of the target section tends to be stable. It can be found that when using the MC model, the surface settlement values at the 10m, 20m, and 30m sections from the entrance of the tunnel are 18.79mm, 19.40mm, and 17.07mm respectively. Under the SS model, the surface settlement values at the 10m, 20m, and 30m sections from the entrance of the tunnel are 22.70mm, 23.64mm, and 22.05mm respectively, which are respectively 20.8%, 21.9%, and 29.2% higher than the calculation results under the MC model. It also shows that the settlement of diatomite is greater when the SS model is adopted and it is more conservative.

### Vault settlement

The change law of the vault settlement of each target section under the calculation conditions of different constitutive models with excavation steps is shown in Figure 11. After the test tunnel is excavated, the change law of vault settlement along the tunnel axis is shown in Figure 12.

In Figure 11, the changing trend of calculation results of the vault settlement about the two constitutive models is basically the same, and the settlement increases rapidly with the progress of the excavation steps. However, after the excavation face passes through the target section, the settlement rate gradually slows down and eventually stabilizes. Under the MC model, the vault settlement values at 10m, 20m, and 30m sections from the tunnel entrance are 22.41mm, 27.04mm, and 29.70mm respectively. While under the SS model, the vault settlement values at 10m, 20m, and 30m sections from the tunnel entrance are 26.58mm, 31.98mm, and 36.07mm, which are 18.6%, 18.3%, and 21.4% larger than the calculation results under the MC model, respectively.

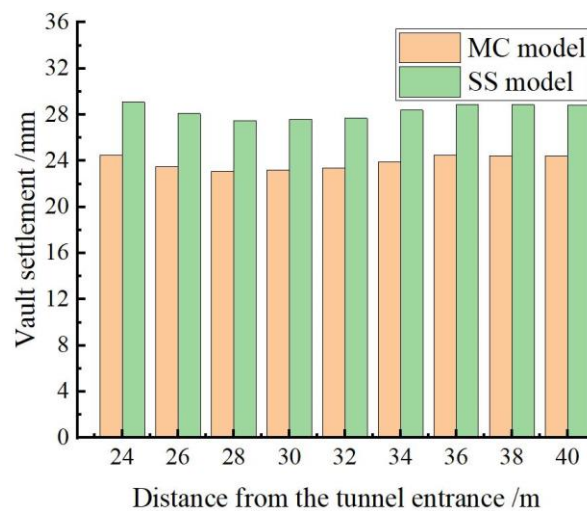
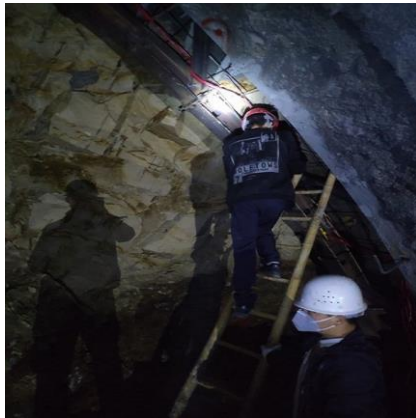


Fig. 12 - Schematic diagram of vault settlement along the tunnel axial direction

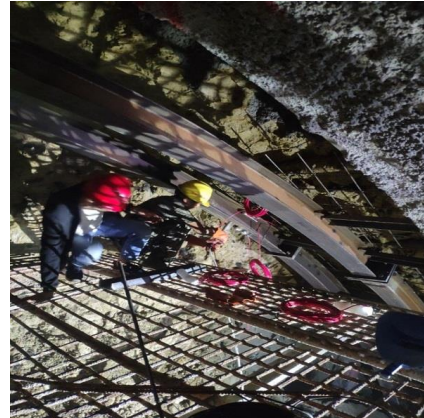
In Fig. 12, after the tunnel excavation, the vault settlement of the MC model and the SS model have similar distribution trends along the tunnel axis, and the vault settlement decreases with the progress of the excavation face. The calculation result of the SS model is even 18% higher than that of the former at the 24m section. Therefore, it is safer to use the SS model to reflect the excavation process about the tunnel in diatomite.

### VERIFICATION OF THE SIMULATION THROUGH ON-SITE MONITORING

To further verify the suitable constitutive model for tunnels in diatomite, the vault settlement of the tunnel on site is monitored and measured. Some on-site monitoring pictures are shown in Figure 13.



(a) Measuring point layout



(b) Instrument installation

Fig. 13 - On-site monitoring pictures

When the on-site monitoring starts, the upper step has excavated to 26m, and the middle step has excavated to 24m. Based on the site conditions, the vault settlement values of measuring point A (12m from the tunnel entrance), measuring point B (15m from the tunnel entrance), and measuring point C (18m from the tunnel entrance) are selected, and the corresponding numerical calculation results of MC model and SS model are extracted and summarized, as shown in Table 3, and the specific layout of measuring points is presented in Figure 14.

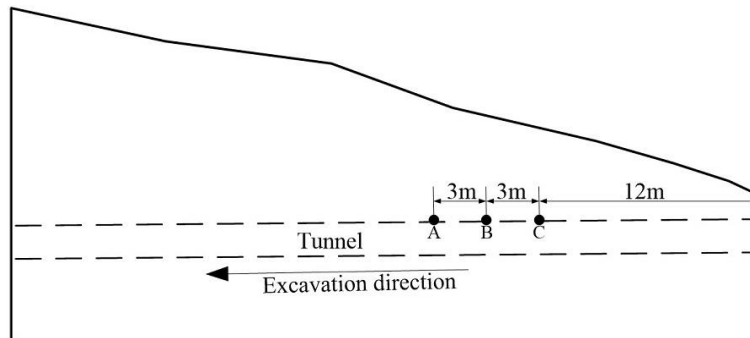


Fig. 14 - Schematic diagram about layout of measuring points along the tunnel axis

Tab. 3 - Comparison of the on-site measured values and numerical simulation values

Name		Vault settlement values of measuring points /mm			
		Measuring point A	Measuring point B	Measuring point C	
Numerical simulation	MC	23.2	25.4	27	
	SS	27.6	29.3	31.9	
On-site measured values		29.8	31.5	33.3	
Percentage difference to measured values		MC: 22.1%    SS: 7.4%	MC:19.3%    SS: 7.1%	MC:18.9%	SS: 4.2%

It can be seen from Table 3 that when the SS model is used for calculation, the maximum percentage difference between the calculated results and on-site monitoring is only 7.4%, and the minimum is 4.2%. While the maximum percentage difference between the MC model and on-site monitoring is 22.1%. Therefore, from the above results, the simulated value under the SS model is closer to the measured value than the MC model. It also shows that for the numerical calculation of tunnel construction in the diatomite layer, the use of the SS model has higher applicability and can well reflect the settlement of surrounding rock. Taking safety into account, since the SS model

considers the influence about softening characteristic of the surrounding rock, the obtained settlement values are greater than the result of the MC model, so the SS model is closer to the actual situation and has a higher safety reserve.

## CONCLUSION

Based on the Feifengshan tunnel, different constitutive models (MC model and SS model) are used to further study the settlement law about the tunnel in diatomite. Then the differences between the on-site test data and the numerical result of these two calculation models is compared and analyzed. The vital conclusions are listed below:

- (1) From the results of the on-site direct shear test of diatomite, it is concluded that the diatomite has obvious strain-softening mechanical characteristics. In the softening stage, the shear force gradually decreases after the peak shear force appears, while the shear displacement continues to increase. In the residual stage, the shear force gradually reaches a stable value, but the shear displacement continues to accumulate.
- (2) By comparing the numerical calculation results about surface settlement and vault settlement of the MC model and the SS model, it is concluded that the settlement change law of the two models with the excavation steps is similar, namely, the settlement increases rapidly with the progress of excavation steps. After the excavation face passes through the target section, the settlement rate gradually slows down and eventually stabilizes. However, it is also found that the settlement value under the SS model is much larger than that of the MC model and it is safer.
- (3) By comparing the settlement values about MC model and SS model with the on-site measured values, it is concluded that the results of the SS model are closer to the measured results than the MC model. The reason is that the MC model does not fully consider the softening characteristics of the material and cannot well reflect the softening characteristics of diatomite. Therefore, the SS model has better applicability for the numerical analysis about tunnel construction in diatomite.

## ACKNOWLEDGMENTS

This work was supported by the National Natural Science Foundation of China (Grant number: 52178395).

## Competing interests

The authors have no relevant financial or non-financial interests to disclose.

## DATA AVAILABILITY

All data, models, and code generated or used during the study appear in the submitted article.

## REFERENCES

- [1] Day, R.B., 1995. Engineering properties of diatomaceous fill. *Journal of Geotechnical Engineering*, Vol. 121, 908 – 910. [https://doi.org/10.1061/\(ASCE\)0733-9410\(1995\)121:12\(908\)](https://doi.org/10.1061/(ASCE)0733-9410(1995)121:12(908))
- [2] Fang, Y.Y., 2019. Study on behavior of Shengzhou diatomite considering structural effects. Master's thesis, Zhejiang University, Hangzhou.
- [3] Han, J.W., 2021. Experimental study and measures on engineering characteristics of diatomite subgrade in Shengzhou. *American Journal of Traffic and Transportation Engineering*, Vol.6, 95-106. <https://doi.org/10.11648/j.ajtte.20210603.14>
- [4] Yang, M.Y., Liu, B., 2021. Study on experimental scheme of different types of pile diatomite foundation treatment for high-speed railway. *Subgrade Engineering*, 85-91. <https://doi.org/10.13379/j.issn.1003-8825.202106004>

- [5] Li, Y., Jiang, Z.Y., Gao, W.S., et al., 2022. Field test study on reinforcement method of diatomite tunnel base. *Subgrade Engineering*, 89-93. <https://doi.org/10.13379/j.issn.1003-8825.202011053>
- [6] Chen, C., 2021. Experimental study on multi-pile reinforcement effect of diatomite foundation for highspeed railway. Master's thesis, Southwest Jiaotong University, Chengdu.
- [7] Yin, J.H. and Graham, J., 1999. Elastic viscoplastic modeling of the time-dependent stress-strain behavior of soils. *Canadian Geotechnical Journal*, Vol. 36, 75-105. <https://doi.org/10.1051/jp4:2005129032>
- [8] Liao, H.J., Su, L.J., Yin, J.H., 2004. 3-D elastic viscoplastic modeling analysis of a diatomaceous soft rock. *Rock and Soil Mechanics*, Vol. 25, 337-341. <https://doi.org/10.16285/j.rsm.2004.03.001>
- [9] Zhang, Y.S., Guo, C.B., Qu, Y.X., et al, 2012. Discovery of swelling diatomite at Tengchong, Yunnan Province and its implication in engineering geology. *Journal of Engineering Geology*, Vol. 20, 266-275.
- [10] Xiang, Q.M, Gao, Y.Q, Su, J.X., et al, 2022. Strata subsidence characteristics of shield tunneling in coastal soft soil area. *Stavební obzor-Civil Engineering Journal*, 31(3), 444-455. <https://doi.org/10.14311/CEJ.2022.03.0033>
- [11] Luo, J.W., Zhang, D.L., Fang, Q., et al, 2021. Mechanical responses of surrounding rock mass and tunnel linings in large-span triple-arch tunnel. *Tunnelling and Underground Space Technology*, Vol. 113, 103971. <https://doi.org/10.1016/j.tust.2021.103971>
- [12] Nguyen, T.T., Do, N.A., Karasev, M.A., et al, 2021. Influence of tunnel shape on tunnel lining behaviour. *Proceedings of the Institution of Civil Engineers-Geotechnical Engineering*, Vol. 174, 355-371. <https://doi.org/10.1680/jgeen.20.00057>
- [13] Qi, W.Q., Yang, Z.Y., Jiang, Y.S., et al, 2021. Structural deformation of existing horseshoe-shaped tunnels by shield overcrossing. *KSCE Journal of Civil Engineering*, Vol. 25, 735-749. <https://doi.org/10.1007/s12205-020-0599-8>
- [14] Zheng, Y., Wu, K., Jiang, Y.J., et al, 2023. Optimization and design of pre-reinforcement for a subsea tunnel crossing a fault fracture zone. *Marine Georesources and Geotechnology*, Vol. 41, 36-53. <https://doi.org/10.1080/1064119X.2021.2009602>
- [15] Pan, H.S., Tong, L.Y., Wang, Z.S., et al, 2022. Effects of soil-cement mixing wall construction on adjacent shield tunnel linings in soft soil. *Arabian Journal for Science and Engineering*, Vol. 47, 13095-13109. <https://doi.org/10.1007/s13369-022-06705-9>
- [16] Nam, S.W., Bobet, A., 2007. Radial deformations induced by groundwater flow on deep circular tunnels. *Rock mechanics and rock engineering*, Vol. 40, 23-39. <https://doi.org/10.1007/s00603-006-0097-4>
- [17] Wang, H.D., He, S.T., 2022. Stability analysis of surrounding rock of shallow-buried subway tunnel with small spacing under different working conditions. *Geotechnical and Geological Engineering*, Vol. 40, 5065-5079. <https://doi.org/10.1007/s10706-022-02200-y>
- [18] Huang, X., Jia, S.D., Yao, C.F., et al., 2022. Settlement analysis of dense buildings under-passed by shield tunnel considering stratum strain softening. *Railway Engineering*, Vol. 62, 111-116.
- [19] Gao, W.S., Wang, L.C., Zhang, H.J., et al., 2021. Analysis of the contribution of face support and primary support to the surface settlement control of shallow tunnel. *Journal of Railway Science and Engineering*, Vol. 18, 720-727. <https://doi.org/10.19713/j.cnki.43-1423/u.t20210097>
- [20] Zhao, Y., Li, X.H., Lu, Y.Y., et al., 2008. Orthogonal design of mechanical parameters in a strain softening model for deeply-buried tunnels. *Journal of Chongqing University*, 716-719.
- [21] Lu, Y.L., Wang, L.G., Yang, F., et al., 2010. Post-peak strain softening mechanical properties of weak rock. *Chinese Journal of Rock Mechanics and Engineering*, Vol. 29, 640-648.
- [22] Sun, C., Zhang, X.D., Liu, J.H., 2013. Application of strain softening model to tunnels based on Hoek-Brown strength criterion. *Rock and Soil Mechanics*, Vol. 34, 2954-2960. <https://doi.org/10.16285/j.rsm.2013.10.029>
- [23] Sun, C., 2013. The research on the strain-softening behavior of the deep joints rock and the interaction between the surrounding rock and the supporting structure. PhD thesis, Liaoning Technical University, Fuxin.
- [24] Su, Y.H., and Zou, Y.H., 2020. Stability analysis of support structure based on HOEK-BROWN strain-softening model. *Journal of Central South University*, Vol. 51, 453-463. <https://doi.org/10.11817/j.issn.1672-7207.2020.02.019>
- [25] Wang, H.B., 2014. Application of strain softening model in numerical simulation of shallow-buried soil tunnel. Master thesis, Huazhong University of Science and Technology, Wuhan.
- [26] Wang, D.Y., Tang, H., Yin, X.T., et al., 2019. Preliminary study on the progressive failure of tunnel-type anchorage based on strain-softening theory. *Chinese Journal of Rock Mechanics and Engineering*, Vol. 38, 3448-3459. <https://doi.org/10.13722/j.cnki.jrme.2017.1497>

- [27] Yang, Y.B., Zheng, J.J., Zhang, R.J., et al., 2015. Comparative study on construction schemes of shallow tunnel in soft rock considering strain-softening behavior. *Journal of Hydraulic Engineering*, Vol. 46, 303-308. <https://doi.org/10.13243/j.cnki.slxb.2015.S1.055>
- [28] Shi, Y.F., Cao, C.W., Tan, Y.F., et al., 2022. Study on dynamic response and long-term settlement of water-saturated weathered soft rocks at the base of subway tunnels. *Modern Tunnelling Technology*, Vol. 59, 86-95. <https://doi.org/10.13807/j.cnki.mt.2022.02.011>
- [29] Qiu, J.L., Fan, F.F., Zhang, C.P., et al., 2022. Response mechanism of metro tunnel structure under local collapse in loess strata. *Environmental Earth Sciences*, Vol. 81, 164. <https://doi.org/10.1007/s12665-022-10256-5>
- [30] Bai, W., Ning, M.Q., Guan, Z.C., 2023. Surface settlement characteristic of shield tunnel excavation under asymmetrical terrain condition. *Journal of Fuzhou University*, Vol. 51, 205-212. <https://doi.org/10.7631/issn.1000-2243.22410>
- [31] Qiao, C.Z., 2021. Stability analysis of tunnel in water-rich and weakly consolidated conglomerate strata based on strain softening model. Master thesis, Beijing Jiaotong University, Beijing.
- [32] Report of in situ direct shear test of diatomite rock on Hangzhou-Shaoxing-Taizhou Railway. Civil Engineering Testing Center of Zhejiang University, 2017, 9-12. (In Chinese)
- [33] Alonso, E., Alejano, L.R., Varas, F., et al., 2003. Ground response curves for rock masses exhibiting strain-softening behaviour. *International Journal for Numerical and Analytical Methods in Geomechanics*, Vol. 27, 1153-1185. <https://doi.org/10.1002/nag.315>